1987ApJ...323...91D

THE ASTROPHYSICAL JOURNAL, 323:91-107, 1987 December 1
© 1987. The American Astronomical Society. All rights reserved. Printed in U.S.A.

THE SPATIAL DISTRIBUTION OF 10 MICRON LUMINOSITY IN SPIRAL GALAXIES

NICHOLAS DEVEREUX[1]
Institute for Astronomy, University of Hawaii
Received 1987 January 10; accepted 1987 May 18

ABSTRACT

New ground-based 10 μm observations of the central region of 133 nearby ($\leq$40 Mpc), infrared, luminous ($\geq 5 \times 10^9\ L_\odot$) galaxies are presented. A first-order estimate of the spatial distribution of infrared emission in galaxies is obtained through a combination of *IRAS* and ground-based photometry. The galaxies studied are primarily noninteracting, permitting an investigation of correlations with Hubble type.

Approximately 40% of the early-type barred spirals in this sample are associated with enhanced 10 μm luminosity in the central ($\sim$1 kpc diameter) region. The underlying luminosity source is attributed to either Seyfert activity or star formation or both. Late-type spirals are different in that luminous central sources are rarely found in either barred or unbarred galaxies. The fact that the bar-central luminosity association is different in early- and late-type spirals indicates that the bulge to disk ratio may be an important parameter determining the central infrared luminosity in barred spirals.

The infrared properties of the "active" early-type barred spirals which most distinguish them from other spiral galaxies in this sample include high central 10 μm luminosity ($\geq 10^9\ L_\odot$), high compactness at 10 μm ($\geq$40%), and a 25 μm color excess ($S_{25\,\mu m}/S_{12\,\mu m} \geq 2.5$). The compactness at 10 μm is significantly correlated with the $S_{25\,\mu m}/S_{12\,\mu m}$ color for early-type spirals. The space density of early-type barred spirals exhibiting a 25 μm color excess is $\sim 10^{-4}$ galaxies Mpc^{-3}, constituting $\sim$10% of all the spiral galaxies in this sample.

Subject headings: galaxies: nuclei — galaxies: photometry — galaxies: structure — infrared: sources

I. INTRODUCTION

There has been considerable interest in the morphological characteristics of galaxies that also exhibit activity in the central region. Indeed, the association of a feature such as a stellar bar in galaxies also exhibiting nuclear activity may be an important clue as to the origin of the activity.

The first results from the *Infrared Astronomical Satellite* (*IRAS*) indicated differences in the infrared properties between barred and unbarred spirals. de Jong *et al.* (1984) noted that in an optically selected sample barred spirals tended to have high-infrared luminosity and hot 100 μm/60 μm color temperature. Hawarden *et al.* (1986*a*) discovered that barred and unbarred galaxies can be partially segregated on the basis of the *IRAS* 25 μm/12 μm flux ratio. Hawarden *et al.* (1986*a*) interpreted the latter result in terms of a burst of nuclear star formation of sufficient luminosity to dominate the *IRAS* 12 and 25 μm emission. However, in a study by Devereux, Becklin, and Scoville (1987) it was shown that the 10 μm luminosity of the central region of an optically selected sample of barred and unbarred galaxies was similar. The result found by Devereux *et al.* was of interest because it did not support the hypothesis proposed by Hawarden *et al.* (1986*a*). The sample of galaxies studied by Devereux *et al.*, however, are of low 40–120 μm luminosity, $L_{FIR} \sim 3 \times 10^9\ L_\odot$: whereas the galaxies studied by Hawarden *et al.* (1966*a*) are biased to high 40–120 μm luminosity, $L_{FIR} \sim 2 \times 10^{10}\ L_\odot$ (Hawarden *et al.* 1986*b*). In this paper, estimates of the central infrared luminosity for galaxies selected on the basis of high-infrared luminosity, $L_{FIR} \geq 3 \times 10^9\ L_\odot$, are presented.

Little is known about the spatial distribution of infrared emission in spiral galaxies; the resolution of the *IRAS* observations permitted an investigation for only a few nearby galaxies of large angular size (Rice *et al.* 1987). In this paper ground-based observations are combined with the *IRAS* data permitting a first-order estimate of the spatial distribution of infrared emission for 149 spiral galaxies exhibiting a wide range in Hubble type and luminosity. It is demonstrated that both the spatial and spectral distribution of emission are significantly correlated with Hubble type. The sample selection and the observations are described in §§ II and III, respectively. The results of both the ground-based and *IRAS* observations are presented in §§ IV and V.

II. THE SAMPLE

The galaxies are selected from a volume-limited catalog compiled by Tully (1987). The catalog (hereafter the *Nearby Galaxies Catalog* [NBG]) includes all known optically bright galaxies with a recession velocity $\leq$3000 km s^{-1}. Galaxy distances have been estimated from a model of the local velocity field (Tully and Shaya 1984). The distance scale is consistent with a Hubble constant of 75 km s^{-1} Mpc^{-1}, and the velocity limit of the sample corresponds to a distance of 40 Mpc.

Galaxies common to both the *IRAS* Point Source Catalog and the NBG catalog have been identified. Since the primary goal of this study is to investigate correlations of infrared properties with the presence of a stellar bar, galaxies not classified according to the de Vaucouleurs, de Vaucouleurs, and Corwin (1976) normal spiral sequence and galaxies for which the bar morphology is unknown are excluded from the sample.

A subsample of 227 galaxies was selected by the following constraints: galactic latitude $|b^{II}| > 20°$, so as to avoid confusion with emission in the Galactic plane; distance $\leq$40 Mpc; and $L_{60\,\mu m} \geq 2.2 \times 10^9\ L_\odot$ ($4\pi D^2 \nu S_\nu$ at 60 μm). The luminosity constraint ensures completeness in the sense that *IRAS* would have detected all galaxies with $L_{60\,\mu m} \geq 2.2 \times 10^9\ L_\odot$ in a volume of radius 40 Mpc. For a typical $S_{100\,\mu m}/S_{60\,\mu m}$ flux ratio

[1] Visiting Astronomer, Infrared Telescope Facility, which is administered by the University of Hawaii under contract to the National Aeronautics and Space Administration.

© American Astronomical Society • Provided by the NASA Astrophysics Data System

1987ApJ...323...91D

of 2.5, the 60 μm luminosity constraint corresponds to a 40–120 μm luminosity, $L_{\rm FIR} = 2.9 \times 10^9\ L_\odot$. An inner distance limit of 15 Mpc was imposed to reduce the fraction of galaxies whose large angular size would require more extensive reduction of the *IRAS* data. A further constraint was the requirement that the emission, observed by *IRAS*, be associated with high confidence to one particular galaxy; thus 32 galaxies with close neighbors, which may also be emitting in the infrared, were excluded from the following analysis. In summary, the sample includes *essentially all known noninteracting galaxies with* $L_{FIR} \geq 2.9 \times 10^9\ L_\odot$ *within a distance approximately twice that to the Virgo cluster.*

III. OBSERVATIONS

New ground-based measurements at 10 μm for 133 galaxies in the right ascension (α) range $22 \leq \alpha \leq 16$ hr and declination (δ) $-40° \leq \delta \leq 60°$ are presented in Table 1. The new observations were obtained with the 3 m NASA Infrared Telescope Facility (IRTF) located at Mauna Kea in Hawaii during the nights of 1986 March 2–6 and November 27–30. The facility gallium-doped germanium bolometer was placed at the Cassegrain focus. The flux calibration was set by measurement of six standard stars whose adopted fluxes are as listed in Table 2. The integration time for each galaxy was 6.6 minutes, yielding a mean (1 σ) sensitivity of 18 mJy.

A 5".5 beam, which for a distance of 20 Mpc corresponds to a projected diameter of $\sim$500 pc, was centered at the peak of the brightest optical emission identified with the Quantex TV guiding system. In a few cases, when the optical emission was diffuse, the beam was placed at the center of the image; such galaxies are indicated in Table 1. The alignment of the infrared and optical beams was checked on a bright infrared star whenever the telescope was moved more than 15°–20° on the sky. The chopper throw was 30" in the N-S direction.

Previously published 10 μm measurements (Scoville *et al.* 1983; Devereux, Becklin, and Scoville 1987; Cizdziel, Wynn-Williams, and Becklin 1985) for 23 of the sample galaxies are also included in Table 1. Eleven of the sample galaxies have been measured previously and are listed in Table 3 to illustrate the good agreement between independent measurements. The *IRAS* measurements for all four bands are also listed in Table 1.

Two requirments for a measurement to be included in the *IRAS Point Source* Catalog discriminate against both faint and extended galaxies. First, the signal-to-noise ratio must be greater than 3.7 for a single measurement to be included in the working survey data base from which the *Point Source Catalog* fluxes are derived. Second, the required point source correlation coefficient is $\geq$87% (*IRAS* Explanatory Supplement 1985). The Addscan software package available at the Infrared Processing and Analysis Center (IPAC) can partially relieve the two limitations outlined above. The sensitivity of the survey may be increased by a factor of $\sim$2 over the typical point source limit by using Addscan to line coadd all the survey scans at a particular position on the sky. Also, since Addscan integrates the detector output over a specified region centered on the source, it is possible to measure the total flux from a slightly extended source.

If the point source flux was a limit, or indicated extended emission, the individual scans were line coadded using the facilities available at IPAC. The flux estimates for 110 galaxies were improved using Addscan and are substituted for the point source measurements as indicated in Table 1. No evidence has been found for any large ($\geq$20%) systematic difference between the point source and the line coadded calibration; thus point source and line coadded fluxes are included in Table 1 and incorporated in the following analysis. Reliable ($\geq 6\ \sigma$) detections in all four *IRAS* bands are currently available for 173 galaxies, 76% of the sample. Ten percent of the sample galaxies that do not have "improved" *IRAS* fluxes are biased to $L_{\rm FIR} < 5.6 \times 10^9\ L_\odot$. Thus the *IRAS* measurements are essentially complete, over the whole sky, for $L_{\rm FIR} \geq 5.6 \times 10^9\ L_\odot$.

The majority of the objects accessible from Mauna Kea during the allocated telescope time were observed. Ground-based 10 μm measurements were obtained for *all* galaxies with $L_{\rm FIR} \geq 5.6 \times 10^9\ L_\odot$ and 70% of the galaxies with $2.9 \times 10^9 \leq L_{\rm FIR} < 5.6 \times 10^9\ L_\odot$.

IV. CORRELATIONS WITH BARRED MORPHOLOGY

To investigate correlations with optical morphology the sample is subdivided on the basis of barred morphology and Hubble type. The barred category includes both B and transition, AB, types on the de Vaucouleurs, de Vaucouleurs, and Corwin (1976) classification scheme. The sample is divided into two categories by Hubble type: early (Sb and earlier) and late types (Sbc and later). The latter segregation is necessary to investigate potential intrinsic differences between spirals of early- and late-type, not necessarily attributable to a stellar bar. The small number of galaxies did not warrant a finer Hubble-type segregation.

The distributions of some observable property such as color or luminosity are compared with a statistical Kolmogorov-Smirnoff (K-S) test, permitting a quantitative estimate of the significance of the difference in that property between barred and unbarred galaxies.

a) Central 10 μm Luminosity

The ground-based 10 μm measurements permit an estimate of the central 10 μm luminosity ($4\pi D^2 \nu S_\nu$) for 156 spiral galaxies. The central 10 μm luminosity $L_{10\,\mu\rm m}$ is evaluated using

$$L_{10\,\mu\rm m}\,(L_\odot) = 8000 S_{10\,\mu\rm m} D^2\ , \qquad (1)$$

where $S_{10\,\mu\rm m}$ is the ground-based measurement in units of millijanskys and the distance is D in units of megaparsecs (Scoville *et al.* 1983).

The histogram of central 10 μm luminosity for early-type spirals is shown in Figure 1; barred galaxies are indicated by shading. The K-S test indicates that the histograms for barred and unbarred galaxies are significantly different at the 97.5% level. The mean central 10 μm luminosity[2] for the histogram of the barred spirals, $L_{10\,\mu\rm m} = 9.7 \times 10^8\ L_\odot$, is 3 times that of the unbarred spirals, $L_{10\,\mu\rm m} = 2.8 \times 10^8\ L_\odot$.

The histograms of central 10 μm luminosity for the late-type spirals is presented in Figure 2. The K-S test indicates that the histograms for barred and unbarred galaxies are not significantly different. Comparison of the distributions of central 10 μm luminosity for early- and late-type spirals illustrates that luminous ($>10^9\ L_\odot$) sources are rarely found in late-type spirals.

The arrows in Figures 1 and 2 indicate 2 σ limits. The K-S test used here does not allow specifically for upper limits. However, application of a more rigorous test, specifically

[2] The mean central 10 μm luminosity includes the 2 σ upper limits at their 2 σ level.

© American Astronomical Society • Provided by the NASA Astrophysics Data System

1987ApJ...323...91D

TABLE 1

OBSERVATIONAL DATA

Name of Galaxy[a]	Type[b]	mJy			Jy		Distance (Mpc)	Compactness at 10 μm[e] (%)	Notes[f]
		$S_{10\mu m}$[c]	$S_{12\mu m}$[d]	$S_{25\mu m}$[d]	$S_{60\mu m}$[d]	$S_{100\mu m}$[d]			
NGC 7817	SABbc	44 ± 32	492	584	5.06	15.14	31.5	<16	...
NGC 134	SABbc	...	2450	2690	22.82	60.82	19.0	...	1
NGC 150	SBbcp	...	660	1660	9.90	19.60	19.2	...	1
NGC 157	SABbc	17 ± 24	1580	2420	18.18	46.61	20.9	<4	1
NGC 289	SBbc	...	410	770	6.07	16.64	19.4	...	1
NGC 337	SBd	4 ± 15	350	820	10.44	19.78	20.7	<12	1,13
NGC 470	SAbc	176 ± 17	591	1100	6.30	11.85	30.5	38	...
NGC 613	SBbc	...	2700	4780	29.82	58.85	17.5	...	1
NGC 701	SBc	-11 ± 29	349	662	6.14	13.31	22.7	<21	...
NGC 908	SAc	45 ± 20	1800	2300	17.73	53.86	17.8	3	1
NGC 922	SBcdp	33 ± 16	240	710	4.91	10.70	37.7	19	1
NGC 986	SBab	...	1440	4170	24.58	54.60	23.2	...	1
NGC 1022	SBa	374 ± 23	801	3283	19.85	26.70	18.5	73	...
NGC 1084	SAc	86 ± 19	2180	3780	31.00	60.41	17.1	5	1
NGC 1087	SABc	60 ± 32	...	...	...	...	19.0	...	2
UGC 2460	SBbc	124 ± 15	160	710	3.80	6.21	34.2	124	1
NGC 1187	SBc	177 ± 21	980	2210	12.61	28.20	16.3	24	1
NGC 1241	SBb	86 ± 26	550	720	4.63	11.54	26.6	19	1
NGC 1309	SAbc	-10 ± 19	440	720	6.22	15.90	26.0	<11	1
NGC 1326	SBO	105 ± 42	312	799	8.19	13.81	16.9	46	...
0331-21	SBbc	60 ± 17	240	1240	9.33	13.30	22.1	42	1
NGC 1365	SBb	363 ± 44	3225	11130	77.75	139.90	16.9	17	3
NGC 1386	SAO	208 ± 26	504	1453	5.82	9.53	16.9	58	4
NGC 1385	SBcd	12 ± 16	1320	2190	18.54	39.06	17.5	<3	1
NGC 1415	SABO/a	-40 ± 31	300	553	5.22	11.88	17.7	<26	...
NGC 1421	SABbc	1 ± 14	930	1710	11.81	25.87	25.5	<4	1
NGC 1511	SAcp	...	...	...	22.31	40.56	15.1	...	...
NGC 1625	SBb	...	...	...	1.06	3.59	38.3	...	...
UGC 3190	SAc	...	...	...	5.54	9.44	25.5	...	...
NGC 1784	SBc	33 ± 25	391	752	3.72	10.88	28.7	<16	1
NGC 1832	SBbc	11 ± 26	681	921	8.23	20.39	23.5	<9	1
NGC 1954	SBc	...	...	...	1.29	4.84	39.3	...	...
NGC 1964	SABb	-8 ± 27	793	1278	9.89	24.61	20.0	<8	1
0550-17	SAcd	0 ± 12	212	229	2.59	7.11	39.0	<13	1
NGC 2139	SABcd	12 ± 25	332	838	7.58	15.50	22.4	<21	1
NGC 2146	SBabp	...	5840	17309	141.30	185.70	17.2	...	...
UGC 3463	SABbc	11 ± 11	188	228	2.34	7.08	38.9	<14	1
NGC 2273	SBa	185 ± 23	456	1371	6.24	9.91	28.4	58	4
NGC 2268	SABbc	...	...	...	4.71	14.04	34.4	...	...
NGC 2608	SBb	...	...	...	2.26	5.75	31.0	...	...
NGC 2633	SBb	...	683	2328	15.88	26.25	33.2	...	...
NGC 2708	SAb	31 ± 20	186	464	2.62	6.96	27.8	<29	1
NGC 2701	SABbcp	...	...	...	1.95	5.69	35.1	...	...
NGC 2712	SBb	26 ± 15	229	269	2.08	6.25	28.6	<16	1
NGC 2750	SABc	75 ± 18	180	571	4.24	8.28	38.4	60	1
NGC 2748	SAbc	...	...	...	6.83	18.84	23.8	...	...
NGC 2776	SABc	-2 ± 12	363	437	3.99	10.33	38.7	<8	1
NGC 2782	SABap	113 ± 12	513	1474	8.32	13.34	37.3	31	5
NGC 2893	SBO/a	57 ± 15	186	649	2.39	4.04	26.8	45	1
NGC 2935	SABbc	7 ± 14	555	620	4.88	12.93	30.6	<6	1
NGC 2967	SAc	3 ± 16	406	506	5.06	14.62	30.9	<9	...
NGC 2964	SABbc	127 ± 15	656	1349	11.66	23.24	21.9	25	...
NGC 3003	SBbc	26 ± 16	142	171	2.88	8.59	24.4	<27	1,6
NGC 2985	SAab	...	...	...	5.45	18.87	22.4	...	...
NGC 3023	SABcdp	-11 ± 18	135	374	2.20	5.15	27.6	<37	1

© American Astronomical Society • Provided by the NASA Astrophysics Data System

1987ApJ...323...91D

TABLE 1—*Continued*

Name of Galaxy[a]	Type[b]	mJy $S_{10\mu m}$[c]	mJy $S_{12\mu m}$[d]	mJy $S_{25\mu m}$[d]	Jy $S_{60\mu m}$[d]	Jy $S_{100\mu m}$[d]	Distance (Mpc)	Compactness at 10 μm[e] (%)	Notes[f]
NGC 3021	SBc	4 ± 14	357	576	3.86	9.90	25.1	<10	...
NGC 3044	SBc	42 ± 16	493	1109	9.17	19.56	20.6	11	6
NGC 3055	SABc	37 ± 15	272	471	3.90	9.40	26.9	17	1
NGC 3067	SABab	56 ± 16	678	1024	8.98	18.53	24.2	10	6
NGC 3066	SABbcp	...	...	...	3.02	5.44	32.4	...	...
NGC 3079	SBm	91 ± 20	2797	4400	43.68	100.35	20.4	4	1
NGC 3166	SABO/a	53 ± 16	332	460	5.48	13.05	22.0	19	6
NGC 3169	SAap	102 ± 16	1306	1239	8.17	23.67	19.7	9	1,6
NGC 3177	SAb	96 ± 16	546	1067	9.04	17.47	21.1	23	6
NGC 3190	SAap	3 ± 16	361	568	3.44	9.93	22.4	<11	6
NGC 3241	SAab	...	...	...	1.17	3.51	37.9	...	...
NGC 3294	SAc	19 ± 13	809	816	5.93	18.27	26.7	<4	1
NGC 3310	SABbcp	100 ± 17	1248	4659	32.96	40.79	18.7	12	5
NGC 3370	SAc	34 ± 13	347	791	3.89	10.69	23.4	13	1
NGC 3430	SABc	-2 ± 15	...	...	2.84	8.01	26.7	...	2
NGC 3437	SABc	52 ± 12	715	1253	11.40	21.40	23.4	9	1
NGC 3445	SABm	...	...	...	2.19	4.27	32.4	...	...
NGC 3504	SABab	402 ± 12	1048	3739	18.91	32.06	26.5	57	5
NGC 3516	SBO	...	455	925	1.73	2.08	38.9	...	3
1107-23	SAbc	18 ± 20	411	768	4.19	10.53	29.5	<12	1
NGC 3568	SBb	-9 ± 14	460	763	7.88	16.72	32.7	<7	1,13
NGC 3583	SBb	56 ± 12	526	711	6.83	17.39	34.0	13	...
NGC 3611	SAap	75 ± 21	351	666	4.96	7.93	27.3	27	...
NGC 3631	SAc	9 ± 16	1300	1621	10.75	29.60	21.6	<3	1,6
NGC 3652	SBcp	...	...	...	2.36	5.78	33.5	...	...
NGC 3655	SAc	16 ± 16	534	783	7.40	18.53	26.5	<7	6
NGC 3665	SAO	...	...	...	1.98	6.10	32.4	...	...
NGC 3672	SAc	33 ± 16	941	1059	9.86	26.36	28.4	4	1
NGC 3683	SBc	57 ± 22	1017	1456	13.80	28.73	28.4	8	...
NGC 3686	SBbc	19 ± 17	373	537	4.29	12.04	23.5	<11	1
NGC 3717	SAab	12 ± 24	1092	1397	13.09	23.52	24.6	<5	1
NGC 3732	SABa	32 ± 12	337	780	4.79	8.38	26.9	13	1
NGC 3783	SBa	502 ± 34	800	2453	3.33	4.93	38.5	90	3
NGC 3780	SAc	...	...	...	1.84	7.74	37.2	...	...
NGC 3810	SAc	-1 ± 16	1757	1976	15.19	38.69	16.9	<2	1,6
NGC 3885	SAa	70 ± 16	511	1446	11.26	14.75	27.8	19	...
NGC 3887	SBbc	0 ± 17	764	871	6.45	16.11	19.3	<5	1
NGC 3888	SABbc	34 ± 12	367	476	4.76	10.96	37.5	11	...
NGC 3893	SABc	28 ± 15	1590	1930	16.68	40.46	17.0	<2	1
NGC 3949	SAbc	-9 ± 22	771	1464	10.11	27.40	17.0	<7	1
NGC 3976	SABc	...	...	...	1.73	6.14	37.7	...	...
NGC 3982	SABbc	4 ± 22	575	981	7.72	17.94	17.0	<10	1,4
NGC 4027	SBdmp	36 ± 13	1028	1097	12.06	26.16	25.6	4	1
NGC 4030	SAbc	40 ± 15	1686	2622	20.48	51.73	25.9	3	1
NGC 4041	SAbc	20 ± 20	...	...	13.64	30.64	22.7	...	...
NGC 4051	SABbc	326 ± 23	1506	2580	11.50	24.55	17.0	27	1,3
NGC 4085	SABc	...	...	...	5.45	14.23	17.0	...	...
NGC 4088	SABcp	23 ± 17	2203	3975	27.66	62.55	17.0	<2	1
NGC 4100	SAc	40 ± 17	777	1289	9.87	23.00	17.0	6	1
NGC 4102	SABb	744 ± 24	1456	6870	47.00	67.27	17.0	84	14
NGC 4152	SABc	47 ± 11	319	529	4.13	9.20	34.5	18	5
NGC 4157	SABb	10 ± 25	2030	2529	18.93	52.13	17.0	<3	1,13
NGC 4162	SAbc	21 ± 9	214	449	2.71	7.54	38.5	13	1
NGC 4194	SBOp	376 ± 28	860	4385	22.50	25.20	39.1	74	5
1212-35	SBc	113 ± 21	345	2239	11.36	17.31	36.5	61	1

© American Astronomical Society • Provided by the NASA Astrophysics Data System

1987ApJ...323...91D

TABLE 1—*Continued*

Name of Galaxy[a]	Type[b]	mJy $S_{10\mu m}$[c]	mJy $S_{12\mu m}$[d]	mJy $S_{25\mu m}$[d]	Jy $S_{60\mu m}$[d]	Jy $S_{100\mu m}$[d]	Distance (Mpc)	Compactness at 10 μm[e] (%)	Notes[f]
NGC 4212	SAbc	47 ± 10	944	1347	7.01	18.56	16.8	6	1,7
NGC 4254	SAc	-3 ± 17	3411	4194	31.25	89.01	16.8	<1	1,7
NGC 4273	SBc	71 ± 14	595	1175	9.73	21.08	35.1	15	...
NGC 4303	SABbc	80 ± 17	3077	3648	35.03	78.01	15.2	3	1,7
NGC 4304	SBb	76 ± 20	496	991	6.87	11.47	36.0	20	1
NGC 4321	SABbc	40 ± 11	2608	2542	21.39	67.69	16.8	2	1,7
1221-34	SAc	-19 ± 33	382	650	3.10	7.50	37.0	<22	1
NGC 4369	SAa	35 ± 15	340	723	5.91	11.16	21.6	14	...
NGC 4385	SBa	126 ± 15	332	1482	4.57	6.14	33.5	61	1,5
NGC 4412	SBbcp	14 ± 15	<247	412	3.17	6.20	35.6	...	1,8,13
NGC 4419	SBa	147 ± 17	545	1460	7.69	17.32	16.8	37	7
NGC 4501	SAb	17 ± 17	1949	3378	19.04	64.43	16.8	<2	1,7
NGC 4526	SABO	59 ± 13	370	556	4.65	16.50	16.8	20	1,7
NGC 4527	SABbc	126 ± 19	2822	3410	34.36	65.33	29.3	5	1
NGC 4532	IBm	2 ± 20	296	947	8.91	16.56	15.5	<20	1,13
NGC 4535	SABc	76 ± 17	1210	1707	12.04	32.26	16.8	8	1,7
NGC 4569	SABab	133 ± 17	1150	2330	9.86	27.82	16.8	15	1,7
NGC 4593	SBb	199 ± 17	371	926	2.76	5.79	39.5	73	3
NGC 4602	SABbc	-4 ± 8	540	502	5.02	13.20	37.9	<3	...
NGC 4654	SABcd	22 ± 17	1240	1820	13.26	41.31	16.8	<3	1,7
NGC 4658	SBc	14 ± 13	296	380	4.82	9.48	35.7	<11	1,13
NGC 4691	SBbp	113 ± 15	717	2439	14.97	21.10	22.5	23	...
NGC 4699	SABb	20 ± 11	...	...	4.61	18.01	25.7	...	9
NGC 4710	SAO	43 ± 13	378	674	5.88	14.52	16.8	14	1,7
NGC 4750	SAab	...	378	386	4.39	13.97	26.1	...	...
NGC 4731	SBcd	...	...	...	2.35	6.14	25.9	...	...
NGC 4775	SAd	5 ± 15	128	293	4.59	9.57	26.6	<31	1
NGC 4781	SBd	21 ± 19	550	652	7.79	17.64	22.5	<8	...
NGC 4793	SABc	28 ± 12	657	1173	11.41	27.21	38.9	5	...
NGC 4814	SAb	...	...	...	1.77	6.48	39.3	...	...
NGC 4808	SAcd	-10 ± 15	678	696	6.69	14.73	20.9	<5	...
NGC 4818	SABab	544 ± 20	854	3899	20.00	25.86	21.5	103	...
NGC 4845	SAa	132 ± 26	437	682	9.29	23.03	15.6	37	...
NGC 4900	SBc	8 ± 21	342	470	5.39	11.86	17.3	<15	...
NGC 4899	SABc	20 ± 12	174	174	2.45	7.45	38.4	<16	1,13
NGC 4902	SBb	7 ± 13	522	473	4.40	11.68	39.2	<6	1
NGC 4947	SBb	...	...	...	2.26	8.22	33.3	...	...
NGC 4961	SBcd	...	...	...	1.16	2.64	39.4	...	...
NGC 4981	SABbc	42 ± 15	451	656	3.22	11.05	27.8	11	1
NGC 4984	SABa	310 ± 23	708	1712	11.18	15.14	21.3	59	...
NGC 4995	SABb	25 ± 20	536	476	4.11	12.15	28.0	<9	1
NGC 5005	SABbc	125 ± 16	1872	2279	23.43	64.49	21.3	8	1,4,6
NGC 5033	SAc	31 ± 16	1770	2100	18.16	51.94	18.7	<2	1,3
NGC 5054	SAb	69 ± 14	616	1040	11.25	27.48	27.3	14	...
NGC 5085	SAc	36 ± 13	732	575	4.47	14.44	28.9	6	1
1322-19	SABcd	...	...	...	1.83	2.70	29.8	...	...
NGC 5161	SABcd	...	...	...	2.19	7.39	33.5	...	...
NGC 5188	SBap	208 ± 25	758	2809	22.44	34.61	32.9	42	...
NGC 5247	SAc	12 ± 12	1784	1654	14.84	37.12	22.2	<2	1
NGC 5290	SBbcp	...	...	...	1.66	5.10	37.8	...	...
NGC 5297	SABb	18 ± 16	...	...	2.15	7.64	37.8	...	...
NGC 5301	SAb	5 ± 16	454	509	2.32	9.00	27.7	<8	1,13
NGC 5347	SBab	...	336	930	1.44	2.59	36.7	...	4
NGC 5350	SBbc	48 ± 11	...	...	2.24	8.25	37.8	...	10
NGC 5371	SABbc	6 ± 13	1025	1128	6.09	18.27	37.8	<3	1

© American Astronomical Society • Provided by the NASA Astrophysics Data System

1987ApJ...323...91D

TABLE 1—*Continued*

Name of Galaxy[a]	Type[b]	mJy $S_{10\mu m}$[c]	mJy $S_{12\mu m}$[d]	mJy $S_{25\mu m}$[d]	Jy $S_{60\mu m}$[d]	Jy $S_{100\mu m}$[d]	Distance (Mpc)	Compactness at 10 μm[e] (%)	Notes[f]
NGC 5383	SBbp	41 ± 12	360	648	5.23	12.60	37.8	14	13
1355-29	SAb	...	...	...	1.88	9.48	37.3	...	...
NGC 5427	SAcp	41 ± 13	1263	1228	...	...	38.1	4	1,11,4
NGC 5448	SABa	...	...	...	1.63	4.98	32.6	...	...
NGC 5464	IBm	...	...	...	2.06	2.66	37.5	...	...
NGC 5480	SAcp	34 ± 12	270	430	3.64	9.75	31.9	16	...
NGC 5595	SABc	23 ± 23	678	722	10.28	18.29	38.5	<8	1,13
NGC 5597	SABcd	69 ± 12	667	1610	9.61	15.62	38.6	14	1,5
NGC 5633	SAb	12 ± 15	301	423	2.69	9.08	37.1	<12	1,13
NGC 5660	SABc	39 ± 13	350	613	4.24	10.30	37.2	14	1
NGC 5665	SBmp	31 ± 10	406	784	6.46	12.59	35.4	10	...
NGC 5678	SABb	68 ± 16	1035	1240	10.24	28.00	35.6	8	1
NGC 5668	SAd	-4 ± 12	185	360	3.30	7.40	26.9	<17	1,13
NGC 5676	SAbc	-13 ± 17	1089	1833	12.83	34.80	34.5	<4	1
NGC 5691	SABap	...	<120	<183	....	....	30.2	...	12
NGC 5713	SABbcp	...	1576	3245	23.62	38.94	30.4	...	1
NGC 5740	SABb	17 ± 10	373	444	3.34	7.41	26.6	<6	1
NGC 5757	SBb	109 ± 17	904	1490	7.92	12.97	39.5	15	1,5
NGC 5775	SBc	30 ± 12	2112	2669	23.51	50.01	26.7	2	1,13
NGC 5792	SBb	...	993	1300	9.76	20.22	30.6	...	1
NGC 5806	SABb	13 ± 15	374	781	3.37	8.80	28.5	<10	1
NGC 5861	SABc	24 ± 16	780	1419	9.90	20.85	28.9	<5	1,13
NGC 5894	SBm	...	...	...	1.09	5.12	38.9	...	...
NGC 5885	SABc	...	...	...	2.53	8.81	30.7	...	...
NGC 5899	SABc	...	518	601	4.45	13.09	39.8	...	1
NGC 5915	SBabp	...	430	1364	10.63	15.56	33.7	...	...
NGC 5921	SBbc	22 ± 11	580	664	4.31	12.07	25.2	5	1
1523-22	SBbc	...	...	...	2.09	7.74	33.6	...	...
NGC 5962	SAc	...	778	962	9.83	22.94	31.8	...	1
NGC 5970	SBc	...	...	...	2.64	9.23	31.6	...	...
NGC 6070	SAcd	...	625	1010	5.82	15.59	31.2	...	1
NGC 6181	SABc	...	507	1043	8.75	19.85	36.7	...	...
NGC 6217	SBbc	...	...	...	10.35	20.50	23.9	...	...
NGC 6643	SAc	...	...	...	10.14	30.95	25.5	...	...
NGC 6667	SABabp	...	...	...	2.70	6.06	39.5	...	...
1911-54	SBc	...	...	...	1.41	5.67	34.7	...	...
NGC 6810	SAa	...	1059	3510	17.84	33.65	25.3	...	...
NGC 6890	SAb	...	...	...	3.66	8.59	31.8	...	4
NGC 6925	SAbc	...	660	710	5.08	14.80	36.6	...	1
NGC 6943	SABcd	...	...	...	1.78	7.95	38.8	...	...
NGC 7083	SAc	...	...	...	4.70	16.69	38.7	...	...
NGC 7125	SABc	...	...	...	2.26	5.16	38.4	...	...
NGC 7126	SAab	...	...	...	2.50	6.95	37.5	...	...
NGC 7184	SBc	...	...	...	2.09	7.93	34.1	...	...
NGC 7205	SAbc	...	...	...	8.95	23.24	20.5	...	...
NGC 7218	SBcd	...	360	570	5.11	11.62	22.0	...	1
NGC 7233	SB0/a	...	...	...	4.00	6.34	22.7	...	...
NGC 7448	SAbc	0 ± 18	411	610	7.62	17.59	30.3	<11	...
NGC 7479	SBc	305 ± 28	1480	4430	12.72	27.58	32.4	29	1
NGC 7497	SBc	24 ± 33	340	350	4.39	14.66	24.1	<23	1
NGC 7496	SBb	...	330	1529	8.42	14.81	20.1	...	4
NGC 7541	SBbc	82 ± 16	922	1567	18.26	39.05	33.4	11	13
NGC 7552	SBab	...	2991	12010	72.52	99.46	19.5	...	5
NGC 7582	SBab	...	1357	6366	47.63	71.49	17.6	...	4
NGC 7590	SAbc	...	...	...	7.27	17.43	17.3	...	4

© American Astronomical Society • Provided by the NASA Astrophysics Data System

1987ApJ...323...91D

TABLE 1—*Continued*

Name of Galaxy[a]	Type[b]	mJy $S_{10\mu m}$[c]	mJy $S_{12\mu m}$[d]	mJy $S_{25\mu m}$[d]	Jy $S_{60\mu m}$[d]	Jy $S_{100\mu m}$[d]	Distance (Mpc)	Compactness at 10 μm[e] (%)	Notes[f]
NGC 7599	SBc	...	...	...	6.04	17.68	20.2	...	...
NGC 7625	SAap	70 ± 18	583	1033	8.98	18.28	23.0	15	13
NGC 7632	SBO	...	312	606	4.27	6.97	19.3	...	...
NGC 7714	SBbp	281 ± 21	497	2814	11.07	10.92	36.9	99	5
NGC 7721	SAc	25 ± 32	290	530	3.91	12.52	26.1	<28	5
NGC 7723	SBb	23 ± 26	450	900	4.46	12.12	23.7	<15	1
NGC 7755	SBc	...	360	630	3.07	9.05	37.0	...	1

[a] Coordinate name used if there is no NGC or UGC number.
[b] Tully (1987) p = peculiar.
[c] Ground-based 10 μm measurement in millijanskys.
[d] *IRAS* fluxes.
[e] Compactness at 10 μm calculated using eq. (2) (see text). "<" indicates 2 σ limit substituted for $S_{10\,\mu m}$ (mJy).
[f] (1) IPAC coadded fluxes; (2) confused, two sources; (3) Seyfert 1 galaxy; (4) Seyfert 2 galaxy; (5) H II nucleus; (6) 10 μm measurement from Devereux, Becklin, and Scoville 1987; (7) 10 μm measurement from Scoville *et al.* 1983; (8) 4 σ limit at 12 μm; (9) 10 μm measurement from Cizdziel, Wynn-Williams, and Becklin 1985; (10) radiation hit—no data available; at 12 and 25 μm; (11) 60 and 100 μm fluxes confused with NGC 5426; (12) 3 σ limits at 12 and 25 μm, and radiation hit at 60 and 100 μm; (13) optical image is diffuse; (14) possible BL Lac.

designed for censored data, is not necessary because the distance distributions of the galaxies in each of the four subsamples are similar ($\langle D \rangle = 27$ Mpc), and the distribution of limits in each are similar, since all of the measurements were made on the same telescope with the same instrumental sensitivity.

b) *Compactness at* 10 μm

The ratio of the ground-based small-beam 10 μm flux to the larger beam *IRAS* 12 μm flux, color corrected to 10 μm, is a measure of the degree to which the central region dominates the *IRAS* 12 μm flux. The percentage, p, of the *IRAS* 12 μm flux contributed by the central region is calculated using

$$p(\%) = S_{10\,\mu m} f_{cc}/S_{12\,\mu m}\,, \qquad (2)$$

where $S_{10\,\mu m}$ is the ground-based IRTF measurement and $S_{12\,\mu m}$ is the *IRAS* measurement in the same units, and f_{cc} is the color correction factor.[3] The compactness at 10 μm, calculated using equation (2), is listed in Table 1.

The histograms of compactness at 10 μm for early- and late-type spirals are presented in Figures 3 and 4, respectively. The K-S test indicates that the histograms for the barred and unbarred early-type spirals are different at ~90% significance level. The difference is attributed to the "tail" of high compactness in the histogram for barred types.

[3] The details of the color correction are given in the Appendix.

TABLE 2

STANDARD STARS AT 10 MICRONS[a]

Name	N
α Aur	−1.94
μ Uma	−1.03
α Boo	−3.17
β Peg	−2.54
α Tau	−3.03
β And	−2.04

[a] Tokunaga 1986.

The majority (93%) of the early-type spirals exhibiting high central 10 μm luminosity ($\geq 10^9\,L_\odot$) are also compact (≥30%) at 10 μm (see Fig. 3). The association of high central 10 μm luminosity with high compactness indicates that the luminosity enhancement is largely confined to the central region. It is thus concluded that ~40% of the early-type barred spirals are associated with an additional component of 10 μm luminosity that is not present in the unbarred spirals.

The K-S test indicates that the histograms of compactness for barred and unbarred late-type spirals (Fig. 4) are not significantly different. Thus enhanced central 10 μm luminosity is observed predominantly in early-type barred spirals.

c) *The IRAS* $S_{25\,\mu m}/S_{12\,\mu m}$ *Ratio*

The histograms of *IRAS* $S_{25\,\mu m}/S_{12\,\mu m}$ ratio for early- and late-type spirals are shown separately in Figures 5*a* and 5*b*, respectively. The histograms are significantly different at

TABLE 3

REPRODUCIBILITY OF 10 MICRON MEASUREMENTS

NGC	$S_{10\,\mu m}$ (mJy) This Paper	$S_{10\,\mu m}$ (mJy) Other	References
3079.....	91 ± 20	80 ± 17	1
		60 ± 24	2
3504.....	410 ± 20	400 ± 50	3
4254.....	<34	<88	4
4303.....	80 ± 17	69 ± 11	5
		83 ± 14	4
4321.....	40 ± 11	<69	4
		34 ± 7	5
4419.....	147 ± 17	111 ± 11	2
4501.....	<34	<52	4
4535.....	76 ± 17	76 ± 15	4
4569.....	133 ± 17	100 ± 18	4
5005.....	125 ± 16	76 ± 12	5
5033.....	31 ± 16	33 ± 12	1

REFERENCES.—(1) Lawrence *et al.* 1985; (2) Willner *et al.* 1985; (3) Rieke 1976; (4) Rieke and Lebofsky 1978; (5) Cizdziel, Wynn-Williams, and Becklin 1985.

© American Astronomical Society • Provided by the NASA Astrophysics Data System

1987ApJ...323...91D

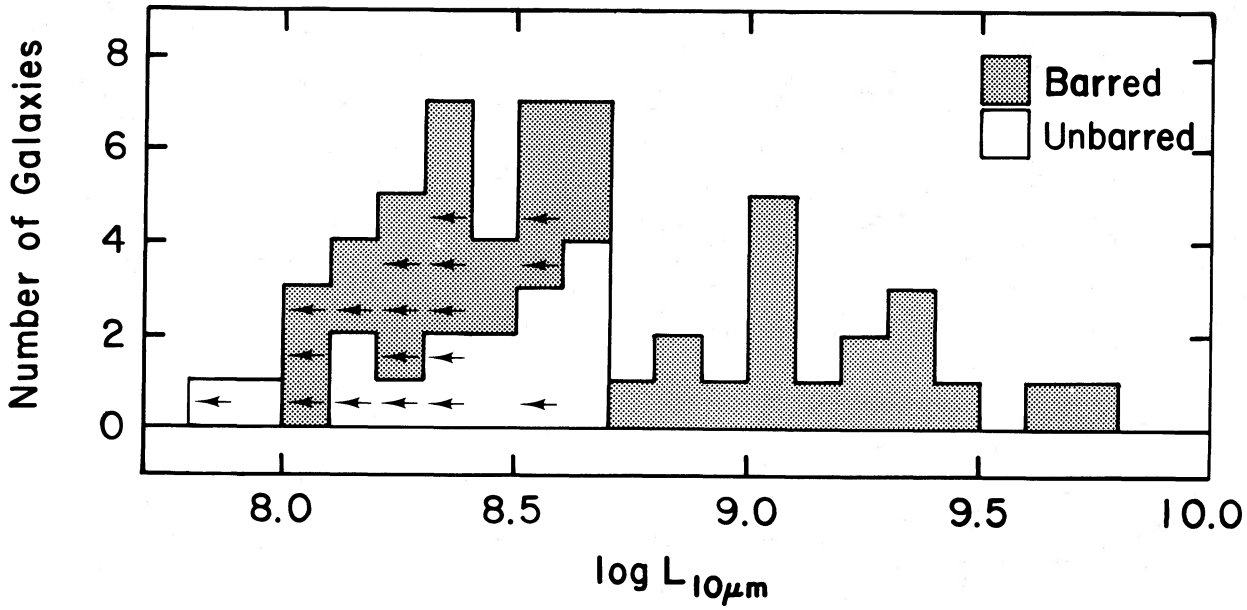

FIG. 1.—Fifty-five early-type spirals (Sb and earlier). Central 10 μm luminosity estimated from ground-based 10 μm observations. In each luminosity interval, the number of barred or unbarred galaxies is given by the shaded or unshaded areas, respectively. Arrows indicate 2 σ upper limits.

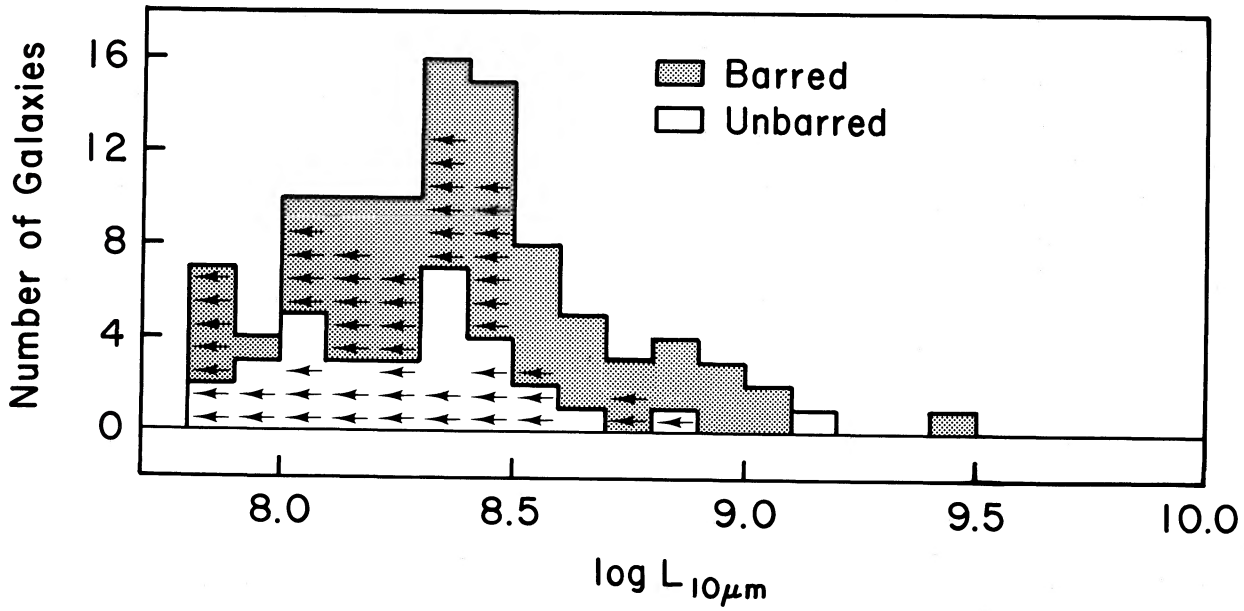

FIG. 2.—Ninety-nine late-type spirals (Sbc and later). Legend as in Fig. 1.

© American Astronomical Society • Provided by the NASA Astrophysics Data System

1987ApJ...323...91D

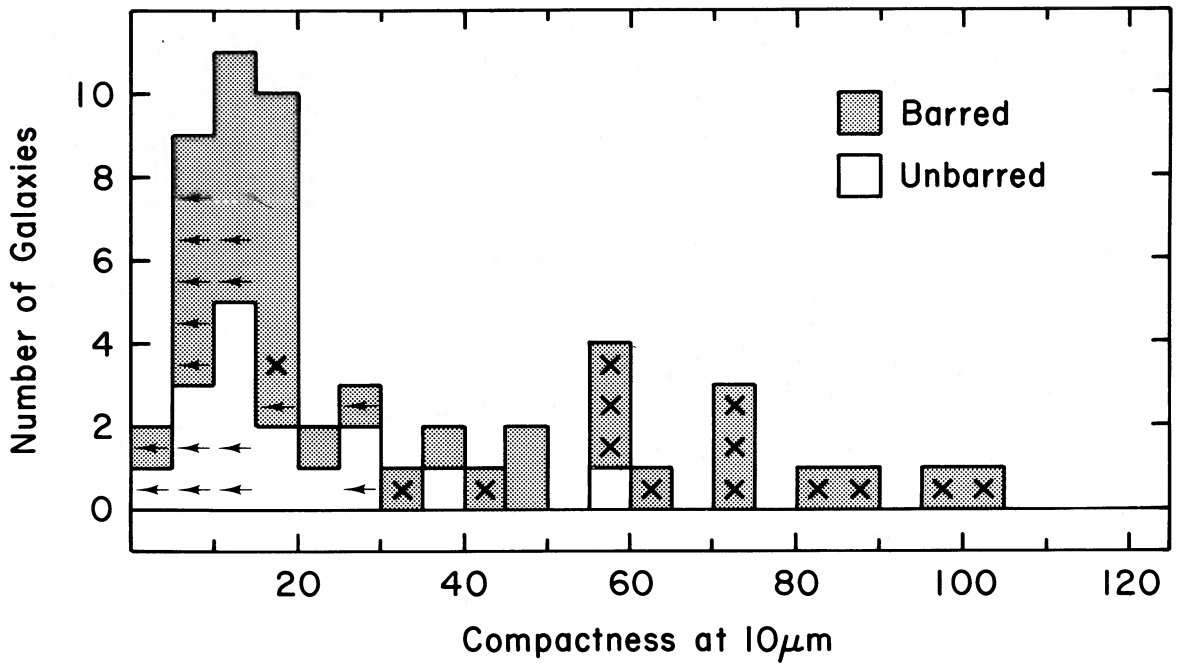

FIG. 3.—Compactness at 10 μm for 55 early-type spirals. Crosses indicate galaxies for which $L_{10\,\mu m}$(center) $\geq 10^9\ L_\odot$. In each compactness interval, the number of barred or unbarred galaxies is given by the shaded or unshaded areas, respectively. Arrows indicate 2 σ upper limits.

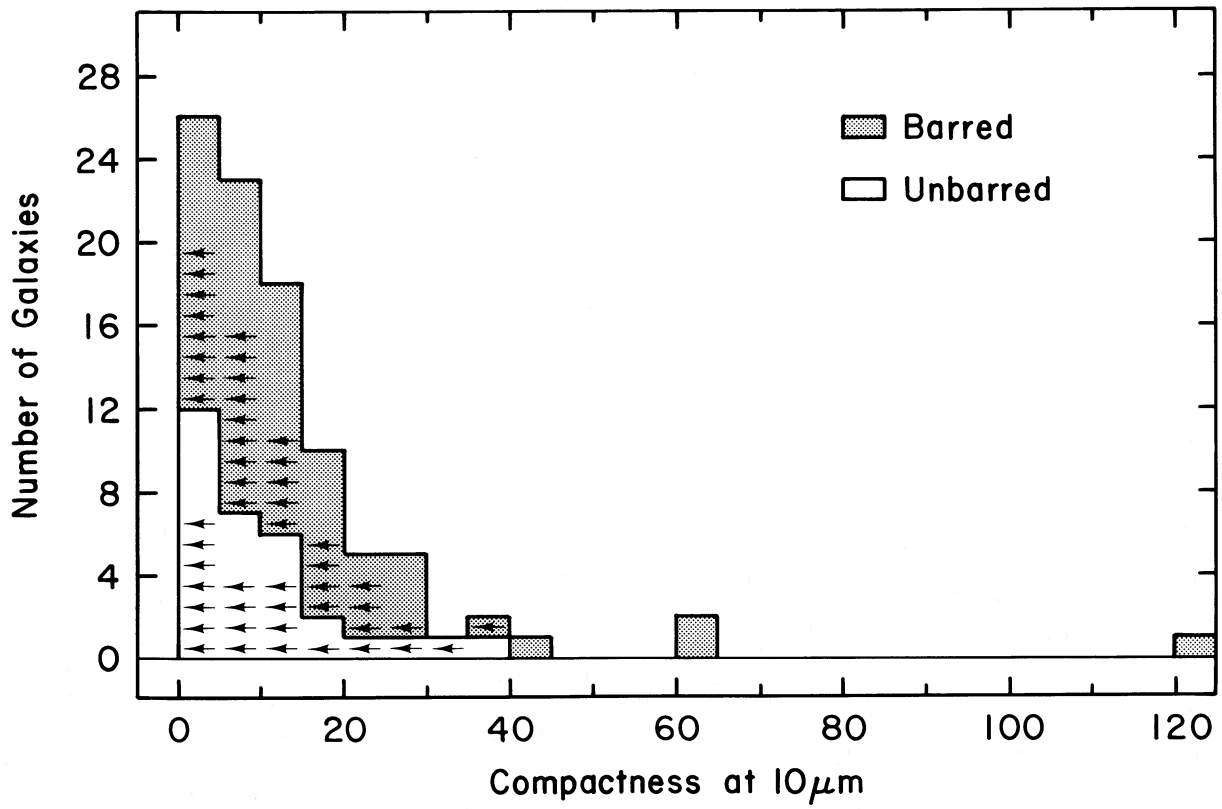

FIG. 4.—Compactness at 10 μm for 94 late-type spirals. Legend as in Fig. 3.

© American Astronomical Society • Provided by the NASA Astrophysics Data System

1987ApJ...323...91D

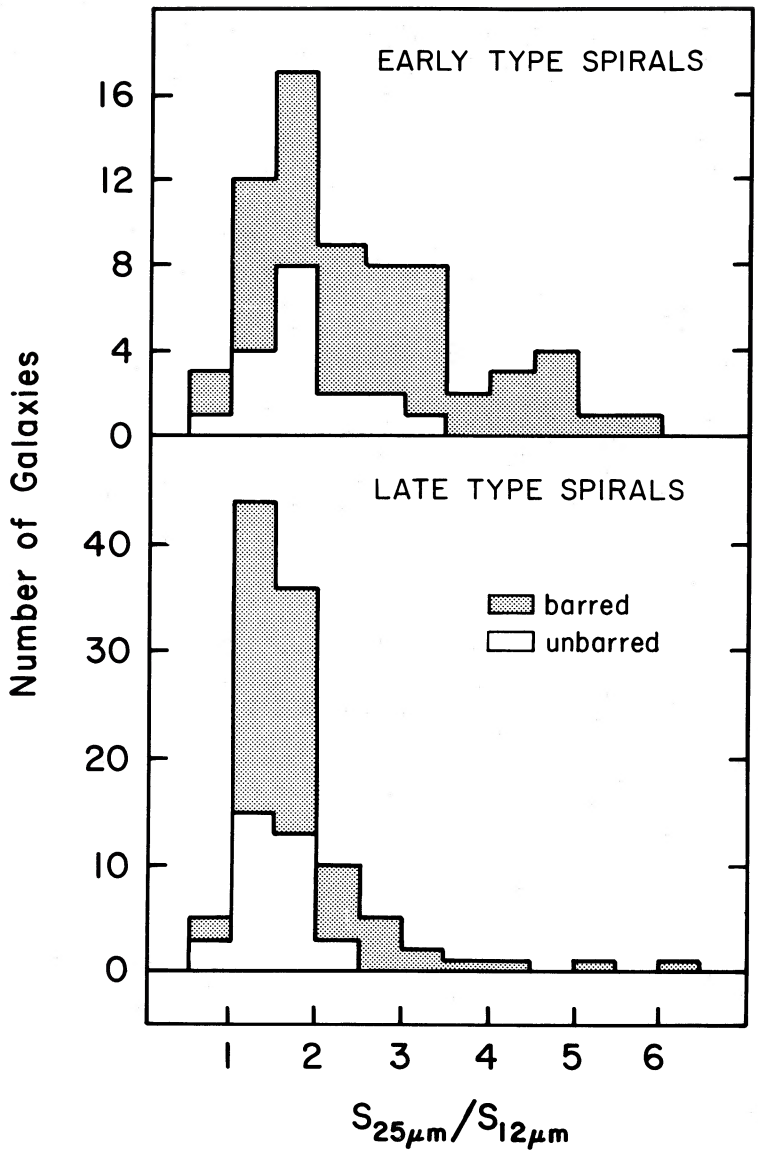

FIG. 5.—(*Top*) *IRAS* $S_{25\,\mu m}/S_{12\,\mu m}$ ratio for early-type spirals. (*Bottom*) *IRAS* $S_{25\,\mu m}/S_{12\,\mu m}$ for late-type spirals. In each color interval the number of barred or unbarred galaxies is given by the shaded or unshaded areas, respectively.

$\geq 99.9\%$ level; the difference is attributed to a larger fraction of the early-type spirals with red $S_{25\,\mu m}/S_{12\,\mu m}$ color.

The K-S test indicates that the distribution of barred galaxies is significantly different to that of unbarred galaxies at the 90% level for early-type spirals. The difference arises in that, among early-type spirals, larger fraction (50%) of the barred galaxies than the unbarred types (17%) exhibit $S_{25\,\mu m}/S_{12\,\mu m} \geq 2.5$. In contrast, the K-S test indicates a less significant ($\leq 90\%$) difference between the barred and the unbarred late-type spirals. These results essentially confirm those of Hawarden *et al.* (1986*a*) but add an important refinement in that the 25 μm color excess is observed predominantly in early-type barred spirals.

d) Correlation between Compactness at 10 μm *and IRAS* $S_{25\,\mu m}/S_{12\,\mu m}$

The compactness at 10 μm is significantly correlated with the *IRAS* $S_{25\,\mu m}/S_{12\,\mu m}$ flux ratio, for early-type spirals (see Fig. 6). The sense of the correlation is that the galaxies exhibiting compact 10 μm emission tend also to exhibit a large $S_{25\,\mu m}/S_{12\,\mu m}$ flux ratio.

It is of interest to consider the possible consequence of a silicate absorption feature on both the estimates of compactness at 10 μm and the correlation presented in Figure 6. One may envisage a scenario in which the compactness at 10 μm is correlated with the optical depth of the silicate absorption feature. Specifically, a silicate absorption feature may suppress the ground-based 10 μm flux, with respect to the *IRAS* 12 μm flux, causing a galaxy to artificially appear extended at 10 μm. In this scenario, galaxies exhibiting compact 10 μm emission would not be expected to exhibit conspicuous silicate absorption features. In the following the full consequences of the silicate absorption feature on the estimates of compactness are investigated.

The 8–15 μm *IRAS* 12 μm filter includes the wavelength interval, 8–13 μm, sampled with the ground-based 10 μm filter.

© American Astronomical Society • Provided by the NASA Astrophysics Data System

1987ApJ...323...91D

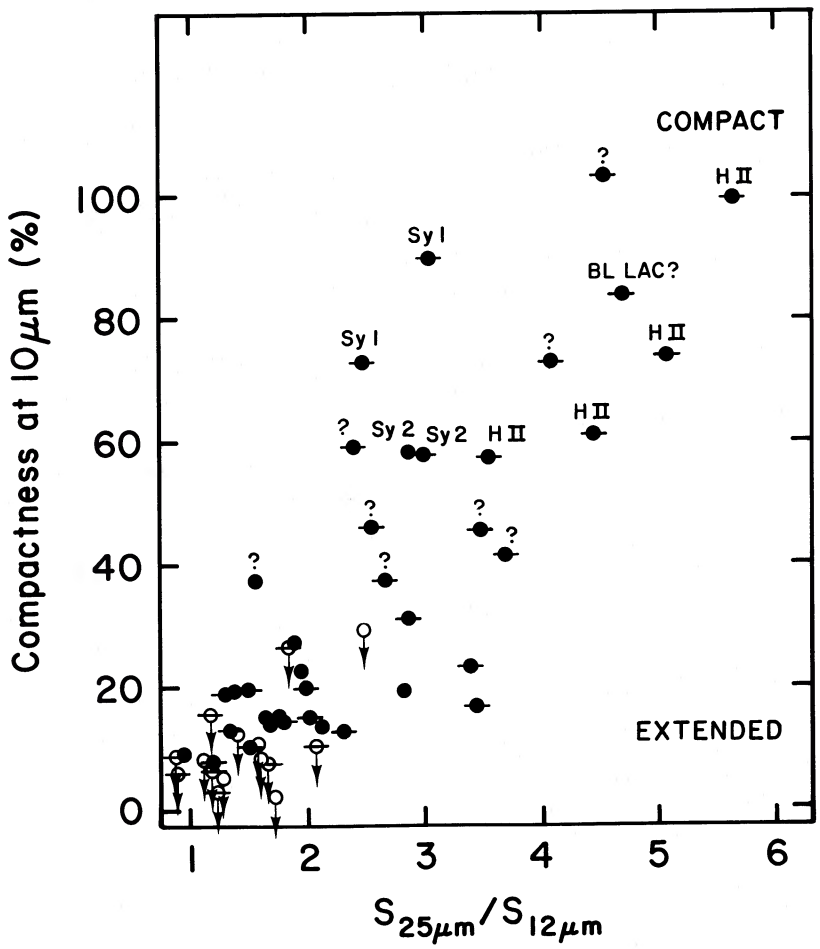

FIG. 6.—Relationship between compactness at 10 μm and *IRAS* $S_{25\,\mu m}/S_{12\,\mu m}$ for early-type spirals. The optical spectral classifications are indicated for galaxies with compactness at 10 μm $\geq$ 30%; Sy 1 $\equiv$ Seyfert 1, Sy 2 $\equiv$ Seyfert 2, H II $\equiv$ H II nucleus, and ? $\equiv$ unknown. Filled circles indicate greater than 2 σ at 10 μm; open circles indicate less than 2 σ limits at 10 μm. Barred morphology indicated by horizontal bars.

The consequence of the "wider" *IRAS* 12 μm filter is to dilute slightly the effect of the silicate absorption with respect to the ground-based filter. If the dilution is not accounted for, the compactness, calculated using equation (2), will be underestimated, causing galaxies to appear more extended than they actually are. Hill, Becklin, and Wynn-Williams (1987) show that for optical depths, $\tau_{9.7\,\mu m} \leq 2$, typical for non-Seyfert galaxies (Phillips, Aitken, and Roche 1984), the compactness is underestimated by $\leq$28% of the value calculated using equation (2), and, even if the optical depth was as high as $\tau_{9.7\,\mu m} = 6$, the compactness is underestimated by less than a factor of 2. Thus, even though the silicate feature may influence the estimate of compactness for some galaxies at the 30% level, it is very unlikely that the silicate feature could reproduce the factor of 10 range in compactness observed for early-type spirals.

Further, a significant silicate feature has been measured for four galaxies exhibiting compact 10 μm emission, galaxies which would not be expected to exhibit a silicate feature under the scenario described above. For NGC 4102, NGC 4194, NGC 4818, and NGC 7714 the optical depths, $\tau_{9.7\,\mu m}$, are approximately 1.6, 1.5, and 0.6 (Becklin and Wynn-Williams, private communication) and 0.3 (Phillips *et al.*) The corresponding values for the compactness at 10 μm are calculated to be 84%, 74%, 103%, and 99%, respectively.

Thus, on the basis of both model calculations and observations it is suggested that the wide range of compactness, illustrated in Figure 6, is unlikely to be correlated with the optical depth of a silicate feature. It is therefore concluded that the correlation presented in Figure 6 reveals an intrinsic relationship between compactness at 10 μm and the *IRAS* $S_{25\,\mu m}/S_{12\,\mu m}$ flux ratio suggesting a distinction between the *IRAS* $S_{25\,\mu m}/S_{12\,\mu m}$ color of early-type spirals for which the 12–25 μm emission is dominated by an "active" central region and those for which the 12–25 μm emission is dominated by a more extended "disk" component.

V. DISCUSSION

There is no doubt that high central 10 μm luminosity is associated almost exclusively with stellar bars for early type spiral galaxies; in fact, stellar bars may be necessary for high central luminosity in noninteracting galaxies. The bar is clearly important, although its actual role is undetermined with the present data. It is of major interest, however, to identify physical parameters that may be important for the bar central luminosity association.

a) The Origin of the High Central Luminosity in "Active" Early-Type Barred Spirals

Early-type barred spiral galaxies of high central 10 μm luminosity ($\geq 10^9\ L_\odot$) are distinguished by a 25 μm color excess and high compactness at 10 μm. In contrast, early-type

© American Astronomical Society • Provided by the NASA Astrophysics Data System

1987ApJ...323...91D

barred and unbarred spirals of low central 10 μm luminosity ($<10^9$ $L_\odot$) exhibit a flat 12–25 μm energy distribution and extended 10 μm emission.

A high percentage (75%) of galaxies exhibiting compact (>50%) emission at 10 μm are also distinguished by bright optical emission lines (see Fig. 6). Seventeen of the early-type spirals are classified on the basis of optical emission lines (Veron-Cetty and Veron 1985, hereafter VCV) and are indicated in Table 1. All but two are barred. The *IRAS* $S_{25\,\mu m}/S_{12\,\mu m}$ ratios, presented in Table 4 for 16 of the early-type spirals exhibiting bright optical emission lines, are similar to the $S_{20\,\mu m}/S_{10\,\mu m}$ ratios determined for Seyfert 1, Seyfert 2, and H II nuclei on the basis of ground-based 10 μm and 20 μm observations by Lawrence *et al.* (1985). The central region may therefore contribute a large fraction of both the *IRAS* 12 μm *and* 25 μm emission for the Seyfert 1, Seyert 2, and H II region nuclei included in Table 4.

On the basis that a 25 μm color excess is a characteristic of Seyfert 1, Seyfert 2, and H II region nuclei and that 50% of the galaxies exhibiting a 25 μm color excess have been classified as such, it is suggested that the origin of the high central 10 μm luminosity observed in early-type barred spirals is Seyfert activity or star formation or both.

Previous studies of the association between stellar bars and nuclear activity have shown that Markarian starburst galaxies do exhibit an excess of barred types, particularly within the Sb-Sbc subgroups (Balzano 1983). The association of Seyfert nuclei with stellar bars, however, is of less significance (Heckman 1978; Simkin, Su, and Schwarz 1980).

Only a small and possibly nonrepresentative subset of the sample galaxies has been classified on the basis of optical emission lines. Thus, in the following, the infrared properties of *all* the early-type spirals in this sample are compared with the infrared properties of Seyfert and starburst galaxies to determine whether Seyfert or starburst activity is associated predominantly with early-type barred spirals.

Most of the galaxies that *IRAS* detected have reliable 60 and 100 μm flux measurements; thus the infrared properties of various classes of galaxies have been characterized largely on the basis of the 40–120 μm luminosity and the $S_{100\,\mu m}/S_{60\,\mu m}$ ratio. Deutsch and Willner (1986) have investigated the 40–120 μm luminosity distribution and 100 μm/60 μm color for Balzano's sample of Markarian starburst galaxies (Balzano 1983). Miley, Neugebauer, and Soifer (1985) have investigated the α(60, 25), α(100, 60) spectral indices and 60 μm luminosity function for galaxies with Seyfert 1 and Seyfert 2 nuclei. In the following the infrared properties of the early-type spiral galaxies, detected in all four *IRAS* bands, are characterized on the basis of (i) the 40–120 μm luminosity and (ii) the *IRAS* colors.

i) 40–120 μm *Luminosity Distributions*

In the following the normalized 40–120 μm luminosity distributions are investigated for early-type spirals segregated on the basis of $S_{25\,\mu m}/S_{12\,\mu m}$ and compactness at 10 μm.

TABLE 4

MEAN $S_{25\,\mu m}/S_{12\,\mu m}$ RATIOS FOR EARLY-TYPE SPIRALS WITH BRIGHT OPTICAL EMISSION LINES

Nuclear Type	$\langle S_{25\,\mu m}/S_{12\,\mu m}\rangle$	Number of Galaxies
Seyfert 1	2.8 ± 0.3	4
Seyfert 2	3.6 ± 0.4	5
H II	3.9 ± 0.5	7

The 40–120 μm luminosity is calculated using equation (3) (*Cataloged Galaxies in the IRAS Survey* 1985),

$$L_{FIR}(L_\odot) = 3.65 \times 10^5 (2.58 S_{60\,\mu m} + S_{100\,\mu m}) D^2 , \quad (3)$$

where the *IRAS* 60 and 100 μm fluxes, in units of janskys, are substituted for $S_{60\,\mu m}$ and $S_{100\,\mu m}$, respectively, and D is the distance in megaparsecs.

The K-S test indicates that the histograms of L_{FIR} for galaxies segregated on the basis of $S_{25\,\mu m}/S_{12\,\mu m}$ are significantly different at the 99.9% level (see Fig. 7). Galaxies with a 25 μm color excess are biased to high luminosity, with respect to those not exhibiting an excess, the median luminosities are $L_{FIR} = 1.8 \times 10^{10}$ $L_\odot$ and $L_{FIR} = 6 \times 10^9$ $L_\odot$, respectively. The median luminosity of galaxies exhibiting a 25 μm color excess is similar to that observed for Seyfert 1, Seyfert 2 (see Miley, Neugebauer, and Soifer 1985), and Markarian starburst galaxies (see Deutsch and Willner 1986).

The histograms of L_{FIR} for galaxies segregated on the basis of compactness at 10 μm are shown in Figure 8. Galaxies with compact 10 μm emission tend to exhibit high L_{FIR} with respect to galaxies with extended 10 μm emission. However, the difference between the histograms in Figure 8 is not as significant as the difference between those in Figure 7. The difference between Figures 7 and 8 is attributed to the fact that a significant percentage (50%) of the most luminous ($L_{FIR} \geq 10^{10}$ $L_\odot$) early-type spiral galaxies, exhibiting a 25 μm color excess, are in the part of the sky not observed at 10 μm and are therefore not included in Figure 8.

ii) *The IRAS Colors*

The distribution of α(60, 25) and α(100, 60) spectral indices for early-type spirals, segregated on the basis of compactness at 10 μm and *IRAS* $S_{25\,\mu m}/S_{12\,\mu m}$ flux ratio, is presented in Figure 9, together with distributions for other galaxy types adapted from a figure presented in Soifer, Houck, and Neugebauer (1987). The spectral indices, α(60, 25) and α(100, 60), are derived from the *IRAS* 60 μm, 25 μm and 100 μm, 60 μm flux densities, respectively. The spectral index, α, is defined $S_\nu \propto \nu^\alpha$.

Galaxies with $S_{25\,\mu m}/S_{12\,\mu m} \geq 2.5$ and high compactness ($\geq$40%) exhibit α(60, 25) and α(100, 60) spectral indices which are different from those observed for galaxies exhibiting $S_{25\,\mu m}/S_{12\,\mu m} < 2.5$ and compactness less than 40%. Further, galaxies with $S_{25\,\mu m}/S_{12\,\mu m} \geq 2.5$ and high 10 μm compactness exhibit α(60, 25) and α(100, 60) spectral indices similar to those observed previously for galaxies with H II type nuclei (see Fig. 9). There is considerable overlap, however, with the spectral indices observed for galaxies with Seyfert 1 and Seyfert 2 nuclei. Few of the sample galaxies exhibit spectral indices characteristic of quasars and BL Lac galaxies (see Fig. 9).

The preceding analysis of *IRAS* luminosities and spectral indices has yielded two important results. First, it is not possible, on the basis of the infrared properties, to distinguish between Seyfert activity and star formation as the origin for the high central 10 μm luminosity observed for early-type spirals. Second, the compactness at 10 μm and the *IRAS* $S_{25\,\mu m}/S_{12\,\mu m}$ flux ratio segregate galaxies similarly in both the far-infrared luminosity and spectral index diagrams. Thus it is concluded that the sample of early-type spiral galaxies with ground-based 10 μm measurements are a representative subset of the larger sample of early-type spiral galaxies with *IRAS* measurements.

b) The Space Density of Active Early-Type Barred Spirals

In addition to luminosities and colors, a population of galaxies may be distinguished by its space density. In the follow-

© American Astronomical Society • Provided by the NASA Astrophysics Data System

1987ApJ...323...91D

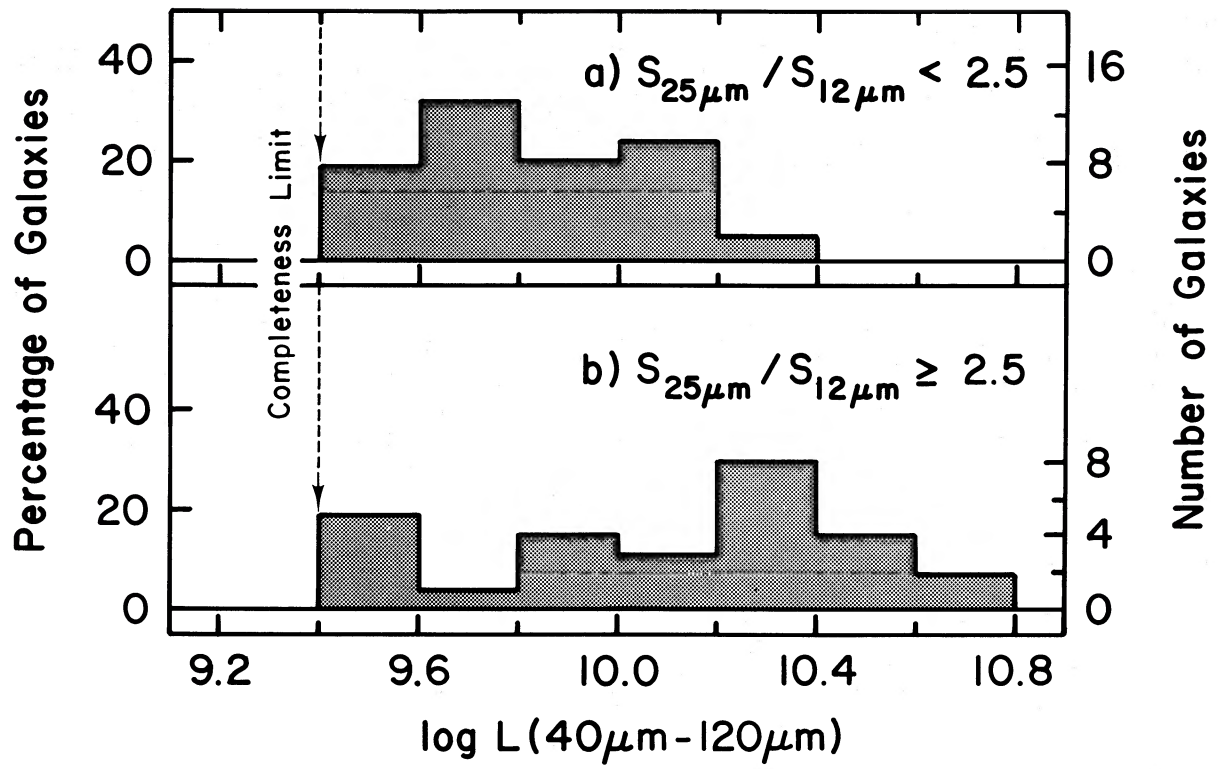

FIG. 7.—(*a*) Normalized 40–120 μm luminosity distributions for early-type spirals with (*a*) $S_{25\,\mu m}/S_{12\,\mu m} < 2.5$. (*b*) $S_{25\,\mu m}/S_{12\,\mu m} \geq 2.5$.

ing, the space density of the "active" early-type barred spirals is calculated and compared with the space density of known Seyfert and Markarian galaxies.

Unfortunately, it is not straightforward to calculate the space density of early-type barred spirals exhibiting enhanced central 10 μm emission because the ground-based 10 μm observations are not complete over the whole sky. However, the correlation between compactness at 10 μm and the *IRAS* $S_{25\,\mu m}/S_{12\,\mu m}$ flux ratio justifies the use of the *IRAS* $S_{25\,\mu m}/S_{12\,\mu m}$ flux ratio as an approximate indicator of compactness at 10 μm. The correlation is useful because the sample of galaxies with *IRAS* fluxes is essentially complete, over the whole sky, for $L_{FIR}/L_\odot \geq 5 \times 10^9$: thus, it is straightforward to calculate directly the space density of early-type barred spirals exhibiting a 25 μm color excess.

The range of 40–120 μm luminosities exhibited by the 24 early-type barred spirals with $S_{25\,\mu m}/S_{12\,\mu m} \geq 2.5$ is $5 \times 10^9 \leq L_{FIR}/L_\odot \leq 5 \times 10^{10}$. The space density of early-type barred spirals exhibiting a 25 μm color excess is $\sim 1 \times 10^{-4}$ galaxies Mpc^{-3}. This may be regarded as a lower limit since the NBG catalog is biased against optically faint ($m_b \geq 12.5$) galaxies which may be bright in the *IRAS* photometric bands. For comparison the space density of Markarian galaxies, in the luminosity interval $5 \times 10^9 \leq L_{FIR}/L_\odot \leq 5 \times 10^{10}$, is $\sim 3.5 \times 10^{-4}$ galaxies Mpc^{-3} (Weedman 1986). The total space density of all Seyfert galaxies is 5×10^{-5} galaxies Mpc^{-3} (Meurs and Wilson 1984); this value has been corrected for a Hubble constant, $H_0 = 75$ km s^{-1} Mpc^{-1} (Felten 1977). The fraction of all Seyfert galaxies with 40–120 μm luminosities in the interval $5 \times 10^9 \leq L_{FIR}/L_\odot \leq 5 \times 10^{10}$ is estimated to be $\sim 70\%$ (Miley, Neugebauer, and Soifer 1985); thus, the space density of Seyfert galaxies in the same luminosity interval is $\sim 3.5 \times 10^{-5}$. The space density estimates are summarized in Table 5. It is of interest to note that the lower limit to the space density of early-type spirals exhibiting a 25 μm color excess is 3 times that of Seyfert galaxies. Thus the number of Seyfert galaxies may be underestimated on the basis of optical and UV excess surveys. Conversely, galaxies exhibiting a 25 μm color excess may constitute a significant fraction of the population of Markarian galaxies.

It is of interest to note that, for this sample, the space density of *all* spiral galaxies in the 40–120 μm luminosity interval $5 \times 10^9 \leq L_{FIR}/L_\odot \leq 5 \times 10^{10}$ is $\sim 1 \times 10^{-3}$ galaxies Mpc^{-3}, in good agreement with the space density of optically bright CfA galaxies in the same luminosity interval (Weedman 1986). Thus galaxies exhibiting infrared characteristics normally associated with Seyfert and starburst activity constitute only 10% of *all* spirals in the same luminosity interval.

TABLE 5

SPACE DENSITY OF VARIOUS CLASSES OF GALAXIES IN THE LUMINOSITY INTERVAL $5 \times 10^9 \leq L_{FIR}/L_\odot \leq 5 \times 10^{10}$

Type	10^{-4} Galaxies/Mpc^3	References
Seyfert	0.35	1, 2
25 μm excess	>1.00	3
Markarian	3.5	4
All spirals	10.0	3

REFERENCES.—(1) Meurs and Wilson 1984; (2) Miley, Neugebauer, and Soifer 1985; (3) This paper; (4) Weedman 1986.

© American Astronomical Society • Provided by the NASA Astrophysics Data System

1987ApJ...323...91D

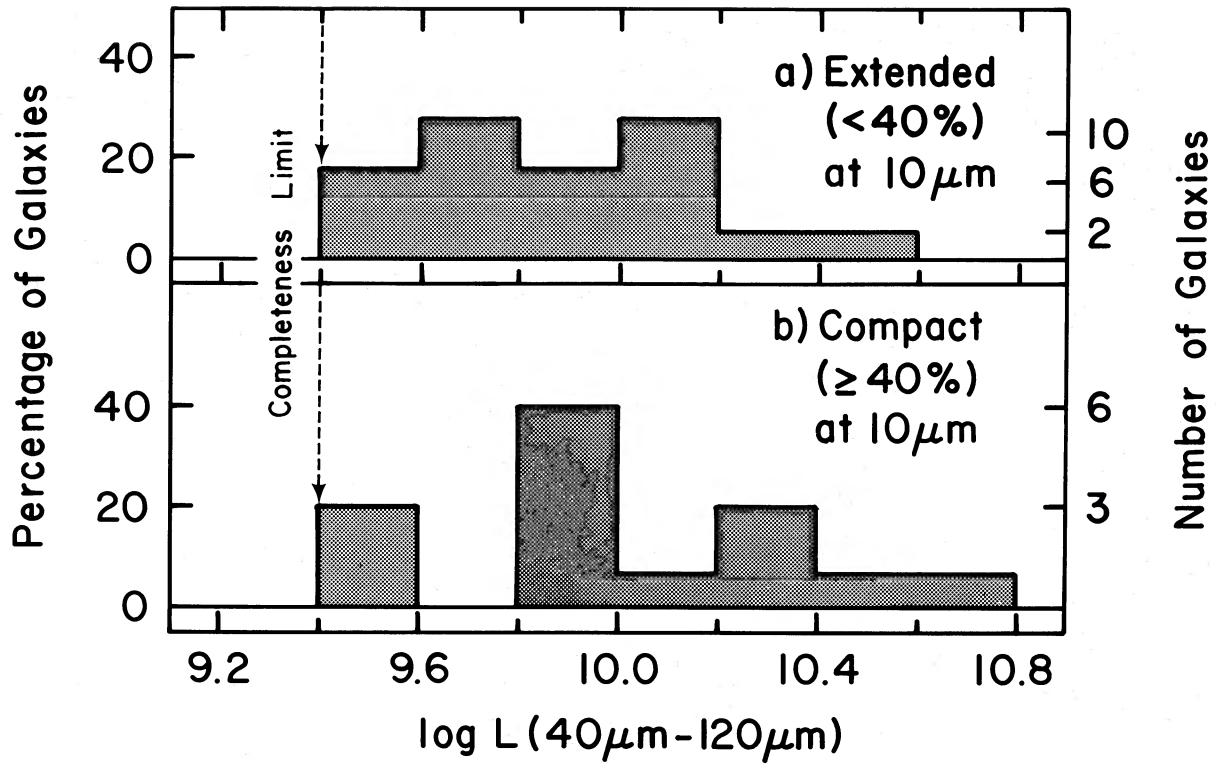

FIG. 8.—Normalized 40–120 μm luminosity distributions for early-type spirals segregated on the basis of compactness at 10 μm. (*a*) Extended, less than 40%; (*b*) compact, ≥40%.

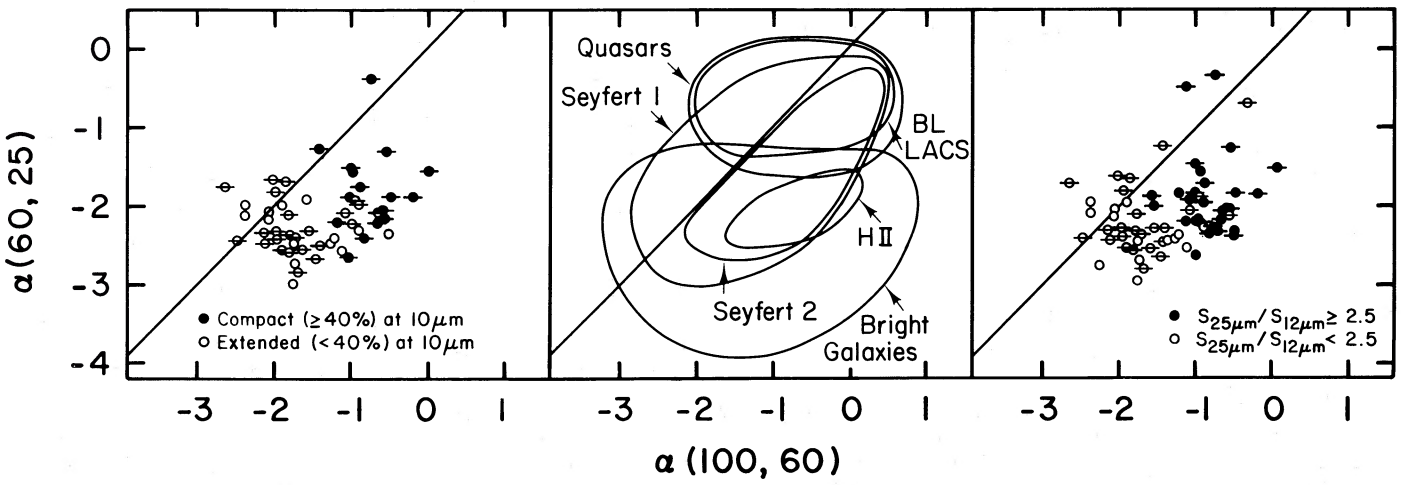

FIG. 9.—α(100, 60) and α(60, 25) spectral indices. (*Left*) Early-type spirals segregated on the basis of compactness at 10 μm. Compact (≥40%) are indicated by filled circles; extended (<40%) by open circles. Barred morphology is indicated by horizontal bars. (*Middle*) Various classes of galaxies adapted, with kind permission, from Soifer, Houck, and Neugebauer (1987). (*Right*) Early-type spirals segregated on the basis of $S_{25\,\mu m}/S_{12\,\mu m} \geq 2.5$ (*filled circles*) and $S_{25\,\mu m}/S_{12\,\mu m} < 2.5$ (*open circles*).

© American Astronomical Society • Provided by the NASA Astrophysics Data System

1987ApJ...323...91D

c) Correlation of Active Early-Type Barred Spirals with Hubble Type

The stellar bar is of less consequence to the central 10 μm luminosity in late-type spirals, indicating that the role of the bar may be different in early- and late-type spirals. A major difference between early- and late-type spirals is the bulge to disk ratio which may influence the relative location of the primary resonances in a barred spiral. The location of the inner Lindblad resonance in particular may be an important parameter determining the observed difference, in central 10 μm luminosity, between early- and late-type spirals.

Combes and Gerin (1985) have simulated the response of an ensemble of molecular clouds to a bar potential and find that a density enhancement, in the form of a ring, may be located near the inner Lindblad resonance. Consequently, the inner Lindblad resonance may be expected to be the site of enhanced star formation activity resulting from cloud-cloud collisions in the ring.

The approximate scale size for an inner Lindblad resonance is set by the distribution of mass in a galaxy and is approximately located at the radius of the "turnover" in the rotation curve. The specific location of the inner Lindblad resonance is determined by the angular velocity of the bar.

The location of the inner Lindblad resonance may be different in early- and late-type spirals. Elmegreen and Elmegreen (1985) note that the bar is short compared with the turnover radius of the rotation curve for late-type spirals. Therefore, if an inner Lindblad resonance exists in late-type barred spirals, it may be located away from the nucleus, near the ends of the bar. In contrast, the bar is long compared with the turnover radius of the rotation curve for early-type spirals. Consequently, the inner Lindblad resonance may be situated well inside the bar and close to the nucleus.

The observation, presented in this paper, that early-type barred spirals exhibit the most luminous nuclei at 10 μm may indicate that the inner Lindblad resonance, and its associated activity, is located within 1 kpc of the nucleus for at least 40% of the early-type barred spirals. NGC 1097 may be a nearby example of an early-type barred spiral exhibiting this phenomenon. The ring of 10 μm emission, observed by Telesco and Gatley (1981), may be associated with an inner Lindblad resonance $\sim$1 kpc from the nucleus. NGC 1365 may be another example of an early-type barred spiral with an inner Lindblad resonance close to the nucleus. On the basis of high spatial resolution kinematical studies Teuben *et al.* (1986) locate the inner Lindblad resonance $\sim$1.5 kpc from the Seyfert nucleus. The observation that the stellar bar is of less consequence to the central 10 μm luminosity in late-type spirals may indicate that the inner Lindblad resonance, and its associated activity, is well removed from the central region.

d) The Correlation of Active Early-Type Barred Spirals with Central 10 μm Luminosity

Only 40% of the early-type barred spirals exhibit high central 10 μm luminosity ($L_{10\,\mu m} \geq 10^9\ L_\odot$); thus the bar is necessary, but not sufficient, for high central 10 μm luminosity. The availability of a gas supply is likely to be an important parameter, in addition to a stellar bar, determining the central luminosity, although the present observations do not constrain this hypothesis.

The result presented in Devereux, Becklin, and Scoville (1987) that barred and unbarred spirals exhibit similar mean 10 μm luminosities is consistent with the results presented in this paper. The histograms of central 10 μm luminosity for barred and unbarred galaxies differ *only* at high ($L_{10\,\mu m} \geq 10^9\ L_\odot$) luminosities in early-type spirals, whereas the galaxies studied by Devereux *et al.* are predominantly of low central 10 μm luminosity, $L_{10\,\mu m} \approx 10^8\ L_\odot$.

VI. SUMMARY AND CONCLUSIONS

Ground-based photometry combined with the *IRAS* photometry has permitted a study of the spatial distribution of infrared emission in spiral galaxies of a wide range in Hubble type and luminosity. Forty percent of the early-type barred spirals are associated with enhanced 10 μm luminosity in the central region. High central 10 μm luminosity is not seen in early-type unbarred or late-type galaxies. It is therefore concluded that stellar bars are important for high central infrared luminosity in early-type spirals.

On the basis of the similarity of the infrared properties to galaxies with Seyfert 1, Seyfert 2, and H II nuclei, the origin of the high central 10 μm luminosity in early-type barred spirals is attributed to star formation or Seyfert activity or both. Approximately 10% of all spiral galaxies in the luminosity interval $5 \times 10^9 \leq L_{FIR}/L_\odot \leq 5 \times 10^{10}$ exhibit infrared characteristics normally associated with Seyfert or starburst activity. The corresponding local space density of galaxies exhibiting infrared characteristics normally associated with Seyfert and starburst galaxies in the luminosity interval $5 \times 10^9 \leq L_{FIR}/L_\odot \leq 5 \times 10^{10}$ is $\sim 10^{-4}$ galaxies Mpc^{-3}.

Stellar bars are of less consequence to the central infrared luminosity in late type spirals. The fact that the bar-central luminosity association is different in early- and late-type spirals may indicate that the bulge to disk ratio is an important parameter determining the central infrared luminosity in barred spirals.

I am most grateful for the invaluable assistance of the staff of the IRTF, in particular Charles Kaminski and David Griep. I would like to thank the staff at IPAC, in particular Walter Rice, Carol Persson, and George Helou. I also thank Gareth Wynn-Williams, Eric Becklin, and Steve Eales for their enthusiastic support of this work. I also thank Andrew Wilson and an anonymous referee for useful comments. This study was supported in part by NSF grant AST 84-18197 and in part under the *IRAS* extended mission program by JPL contract 957695.

APPENDIX A

The following procedure has been adopted to calculate a blackbody temperature from the *IRAS* $S_{12\,\mu m}/S_{25\,\mu m}$ ratio and extrapolate the *IRAS* 12 μm flux to a 10 μm flux. It is shown that the color correction factor, f_{cc}, is related to $S_{25\,\mu m}/S_{12\,\mu m}$ by a simple linear function.

© American Astronomical Society • Provided by the NASA Astrophysics Data System

1987ApJ...323...91D

The *IRAS* photometric data is derived by assuming an intrinsic energy distribution $S_\nu \propto \nu^{-1}$. The assumed intrinsic energy distribution, however, is not representative of the energy distributions observed for galaxies. In this paper it is assumed that over a restricted frequency interval the intrinsic energy distribution of galaxies is best represented by blackbody emission characterized by a single temperature, T_{BB}.

The *IRAS* fluxes must be color corrected in order to be consistent with the assumed intrinsic energy distribution. Following the *Cataloged Galaxies in the IRAS Survey*,

$$\frac{S_{25\,\mu m}}{S_{12\,\mu m}}\,(\text{intrinsic}) = \frac{S_{25\,\mu m}}{S_{12\,\mu m}}\,(\text{quoted})\,\frac{K_{12\,\mu m}}{K_{25\,\mu m}}\,, \tag{A1}$$

where $K_{12\,\mu m}$ and $K_{25\,\mu m}$ are the color correction factors at 12 and 25 μm, respectively and are listed, as a function of T_{BB}, in *Cataloged Galaxies in the IRAS survey*.

Point source and Addscan fluxes are substituted for "quoted" *IRAS* fluxes. An iteration procedure, identical to that described in Castelaz, Sellgren, and Werner (1987), is used to determine the color corrected, *IRAS* $S_{25\,\mu m}/S_{12\,\mu m}$(intrinsic), ratio. The Planck function is used to calculate a temperature T_{BB} from $S_{25\,\mu m}/S_{12\,\mu m}$(intrinsic).

The color-corrected 12 μm flux, $S_{12\,\mu m}$(intrinsic), is calculated using

$$S_{12\,\mu m}(\text{intrinsic}) = \frac{S_{12\,\mu m}(\text{quoted})}{K_{12\,\mu m}}\,. \tag{A2}$$

The *IRAS* color corrected 12 μm flux is extrapolated to a monochromatic 10 μm flux assuming that a blackbody of temperature T_{BB} characterizes the 10–25 μm emission. Thus $S_{10\,\mu m}/S_{12\,\mu m}$(intrinsic) is determined by the Planck function,

$$IRAS\ S_{10\,\mu m}(\text{intrinsic}) = \alpha IRAS\ S_{12\,\mu m}(\text{intrinsic})\,, \tag{A3}$$

where α is the ratio of $S_{10\,\mu m}/S_{12\,\mu m}$ for a blackbody of temperature T_{BB}.

Equations (A2) and (A3) are combined to yield an expression relating the extrapolated 10 μm flux to the quoted *IRAS* 12 μm flux,

$$IRAS\ S_{10\,\mu m}(\text{intrinsic}) = IRAS\ S_{12\,\mu m}(\text{quoted})\,\frac{\alpha}{K_{12\,\mu m}}\,. \tag{A4}$$

It is assumed that the intrinsic energy distribution of the emission from the central region of galaxies is characterized by the same T_{BB} as derived from the *IRAS* $S_{12\,\mu m}/S_{25\,\mu m}$ ratio. The energy distribution of the standard stars used to calibrate the ground-based 10 μm measurements are characterized by T_{BB} much larger than is calculated for galaxies. The ground-based 10 μm measurements must therefore be color corrected to a monochromatic 10 μm flux. The color correction factors, β, appropriate to the IRTF 10 μm filter are listed in Tokunaga (1986). The observed and intrinsic ground-based 10 μm fluxes are related by

$$S_{10\,\mu m}(\text{intrinsic}) = \beta S_{10\,\mu m}(\text{observed})\,. \tag{A5}$$

Combining equations (A4) and (A5), we obtain

$$\frac{S_{10\,\mu m}(\text{intrinsic})}{IRAS\ S_{10\,\mu m}(\text{intrinsic})} = \frac{K_{12\,\mu m}\,\beta}{\alpha}\,\frac{S_{10\,\mu m}(\text{observed})}{IRAS\ S_{12\,\mu m}(\text{quoted})}\,; \tag{A6}$$

the quantity $(K_{12\,\mu m}\,\beta)/\alpha$ is identified with f_{cc} in equation (2) (see text).

The values of K_{12}, α, β, and f_{cc} are listed as a function of *IRAS* $S_{25\,\mu m}/S_{12\,\mu m}$(quoted) and T_{BB} in Table 6 and shown graphically in Figure 10.

The relationship between *IRAS* $S_{25\,\mu m}/S_{12\,\mu m}$ and f_{cc} is well represented by a straight line of equation

$$f_{cc} = [0.12 S_{25\,\mu m}/S_{12\,\mu m}(\text{quoted})] + 1.04\,. \tag{A7}$$

The color correction, f_{cc}, used in this paper is calculated using equation (A7).

TABLE 6

COLOR CORRECTIONS

IRAS $\frac{S_{25\,\mu m}}{S_{12\,\mu m}}$ (quoted)	T_{BB} (K)	$K_{12\,\mu m}$	α	β	f_{cc}
0.91	362	0.98	0.87	1.06	1.19
2.22	233	0.85	0.61	1.00	1.39
3.44	197	0.83	0.51	0.96	1.56
4.56	179	0.83	0.45	0.91	1.68
5.48	167	0.84	0.41	0.87	1.78
6.63	159	0.84	0.38	0.84	1.86

© American Astronomical Society • Provided by the NASA Astrophysics Data System

1987ApJ...323...91D

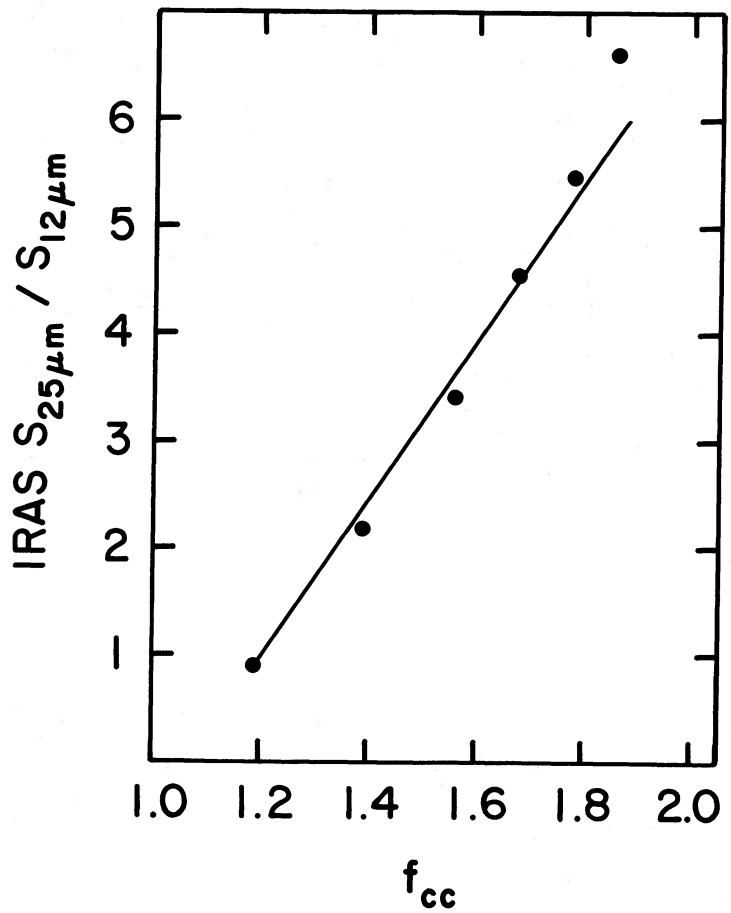

FIG. 10.—Relationship between *IRAS* $S_{25\,\mu m}/S_{12\,\mu m}$ and the color correction f_{cc}. Points are from Table 6. The equation of the straight line is $f_{cc} = [0.12\,S_{25\,\mu m}/S_{12\,\mu m}(\text{quoted})] + 1.04$.

REFERENCES

Balzano, V. A. 1983, *Ap. J.*, **268**, 602.
Castelaz, M. W., Sellgren, K., and Werner, M. W. 1987, *Ap. J.*, **313**, 853.
Cataloged Galaxies and Quasars in the IRAS Survey. 1985, prepared by C. J. Lonsdale, G. Helou, J. C. Good, and W. Rice (Pasadena: Jet Propulsion Laboratory).
Cizdziel, P. J., Wynn-Williams, C. G., and Becklin, E. E. 1985, *A.J.*, **90**, 731.
Combes, F., and Gerlin, M. 1985, *Astr. Ap.*, **150**, 327.
de Jong, T., Clegg, P. E., Soifer, B. T., Rowan-Robinson, M., Habing, H. J., Houck, J. R., Aumann, H. H., and Raimond, E. 1984, *Ap. J. (Letters)*, **278**, L67.
Deutsch, L. K., and Willner, S. P. 1986, *Ap. J. (Letters)*, **306**, L11.
de Vaucouleurs, G., de Vaucouleurs, A., and Corwin, H. G., Jr. 1976, *Second Reference Catalogue of Bright Galaxies* (Austin: University of Texas Press).
Devereux, N. D., Becklin, E. E., and Scoville, N. Z. 1987, *Ap. J.*, **312**, 529.
Elmegreen, B. G., and Elmegreen, D. M. 1985, *Ap. J.*, **288**, 438.
Felten, J. E. 1977, *A.J.*, **82**, 861.
Hawarden, T. G., Fairclough, J. H., Joseph, R. D., Leggett, S. K., and Mountain, C. M. 1986*a*, in *New Light on Dark Matter*, ed. F. P. Israel (Dordrecht: Reidel), p. 455.
Hawarden, T. G., Mountain, C. M., Leggett, S. K., and Puxley, P. J. 1986*b*, *M.N.R.A.S.*, **221**, 41P.
Heckman, T. M. 1978, *Pub. A.S.P.*, **90**, 241.
IRAS Catalog and Atlases: Explanatory Supplement. 1985, ed. C. A. Beichman, G. Neugebauer, H. J. Habing, P. E. Clegg, and T. J. Chester (Washington, DC: US Government Printing Office).
Hill, G. J., Becklin, E. E., Wynn-Williams, C. G. 1987, in preparation.
Lawrence, A., Ward, M., Elvis, M., Fabbiano, G., Willner, S. P., Carleton, N. P., and Longmore, A. 1985, *Ap. J.*, **291**, 117.
Meurs, E. J. A., and Wilson, A. S. 1984, *Astr. Ap.*, **136**, 206.
Miley, G. K., Neugebauer, G., and Soifer, B. T. 1985, *Ap. J. (Letters)*, **293**, L11.
Phillips, M. M., Aitken, D. K., and Roche, P. F. 1984, *M.N.R.A.S.*, **207**, 25.
Rieke, G. H. 1976, *Ap. J. (Letters)*, **206**, L15.
Rieke, G. H., and Lebofsky, M. J. 1978, *Ap. J. (Letters)*, **220**, L37.
Rice, W. L., *et al.* 1987, in preparation.
Scoville, N. Z., Becklin, E. E., Young, J. S., and Capps, R. W. 1983, *Ap. J.*, **271**, 512.
Simkin, S. M., Su, H. J., and Schwarz, M. P. 1980, *Ap. J.*, **237**, 404.
Soifer, B. T., Houck, J. R., and Neugebauer, G. 1987, *Ann. Rev. Astr. Ap.*, in press.
Telesco, C. M., and Gatley, I. 1981, *Ap. J. (Letters)*, **247**, L11.
Teuben, P. J., Sanders, R. H., Atherton, P. D., and Van Albada, G. D., 1986, *M.N.R.A.S.*, **221**, 1.
Tokunaga, A. T. 1986, *IRTF Photometry Manual* (Honolulu: University of Hawaii, Institute for Astronomy).
Tully, R. B. 1987, *The Nearby Galaxies Catalog*, (Cambridge: Cambridge University Press), in press (NBG).
Tully, R. B., and Shaya, E. J. 1984, *Ap. J.*, **281**, 31.
Veron-Cetty, M. P., and Veron, P. 1985, *Catalogue of Quasars and Active Nuclei* (2d ed.; VCV).
Weedman, D. W. 1986, in *Proc. 2nd Internat. IRAS Conf. Star Formation in Galaxies*, Pasadena, California.
Willner, S. P., Elvis, M., Fabbiano, G., Lawrence, A., and Ward, M. J. 1985, *Ap. J.*, **299**, 443.

NICHOLAS DEVEREUX: Institute for Astronomy, 2680 Woodlawn Drive, Honolulu, HI 96822

© American Astronomical Society • Provided by the NASA Astrophysics Data System